ELSEVIER

Polymer 43 (2002) 6993–7001

polymer

www.elsevier.com/locate/polymer

On compatibilization and toughening of a copolyester with a maleated thermoplastic elastomer

Zhong-Zhen Yu[a,b,*], Ming Lei[a], Yuchun Ou[a], Guisheng Yang[a]

[a]*State Key laboratory of Engineering Plastics, Center for Molecular Science, Institute of Chemistry, Chinese Academy of Sciences, P.O. Box 2709, Beijing 100080, People's Republic of China*

[b]*Center for Advanced Materials Technology, School of Aerospace, Mechanical and Mechatronic Engineering (J07), The University of Sydney, Sydney, NSW 2006, Australia*

Abstract

A maleated thermoplastic elastomer (TPEg) was prepared from maleic anhydride, grafting a mixture of polyethylene–octene elastomer and semi-crystalline polyolefin plastic (60/40 by weight) in a twin screw extruder. The non-grafted version (TPE) of the mixture was also prepared under the same processing conditions. The TPEg was employed to compatibilize and toughen amorphous copolyester PETG/TPE blends. The addition of the TPEg improves the compatibility between PETG and the TPE and results in fine dispersion of the TPE in the PETG matrix. At a fixed dispersed phase content of 15 wt%, a sharp brittle–ductile transition takes place, when the TPEg content in the dispersed phase increases from 20 to 30 wt%, namely, the TPEg content in the blends increases just from 3 to 4.5 wt%. After the brittle–ductile transition, the blends are maintained at super-tough level with notched impact strength more than twenty-fold higher than that of pure PETG plastic. The influence of the TPEg content on fractography of the PETG/TPE blends was also investigated. When the TPEg content in dispersed phase is below 20 wt%, the impact fracture surface shows a small area of slow crack growth region and numerous feather-like markings in fast crack growth region, indicating a brittle failure mode. While the TPEg content in the dispersed phase is above 30 wt%, the impact fracture surface exhibits drastically enlarged slow crack growth region and some parabolic markings in the fast crack growth region. Massive cavitation and extensive matrix shear yielding are predominant mechanisms of the impact energy dissipation upon impact testing.

Keywords: Compatibilization; Copolyester; Polyethylene–octene copolymer

1. Introduction

Polymer toughening has always been one of the important topics of material science and has made considerable progress. Numerous approaches have been developed to toughen engineering plastics such as nylon 6, nylon 66, polybutylene terephthalate (PBT) and polyethylene terephthalate (PET). The tougheners used were usually maleic anhydride or glycidyl methacrylate grafted polyolefin elastomers [1–8]. Although they greatly improved the notched impact strength of engineering plastics, the tensile strength and modulus were largely reduced due to the addition of the low modulus elastomers [7,8]. In a previous work [9], we prepared a maleated thermoplastic elastomer (TPEg), which is a maleic anhydride grafted mixture of polyethylene–octene elastomer (POE) and semi-crystalline polyolefin plastic (60/40 by weight). The TPEg was found to be very efficient for toughening nylon 6 [9,10]. Morphological observations showed that the TPEg was dispersed in nylon 6 matrix as a core-shell structure with the semi-crystalline polyolefin plastic being the core and the POE being the shell [9]. Because of its 40 wt% polyolefin plastic content, the TPEg has a lower melt viscosity and a finer dispersion in nylon 6 matrix than the maleic anhydride grafted polyethylene–octene elastomer (POEg) prepared with the same grafting conditions.

Poly(ethylene glycol-*co*-cyclohexane-1,4-dimethanol terephthalate) (PETG) is an amorphous copolyester. Different from PET, it does not undergo crystallization on heating or on plasticization by the dissolved species; the comonomer, cyclohexanedimethanol, is responsible for the completely amorphous nature of this polymer. PETG offers a range of processing parameters broader than that of normal crystallizable polymers and is useful, especially for

* Corresponding author. Address: Center for Advanced Materials Technology, School of Aerospace, Mechanical and Mechatronic Engineering (J07), The University of Sydney, Sydney, NSW 2006, Australia. Tel.: +61-2-9351-7149; fax: +61-2-9351-3760.

E-mail address: zhongzhen.yu@aeromech.usyd.edu.au (Z.-Z. Yu).

0032-3861/02/$ - see front matter
PII: S0032-3861(02)00547-5

obtaining high clarity amorphous moulding. In the past literatures, the research on PETG was mainly focused on physical and mechanical properties of PETG and its blends. Kattan and co-workers [11] studied strain-induced crystallization in uniaxially drawn PETG plates. The crystalline phase could appear as an annealing from the glassy state or by a stretching at high draw ratio. The crystalline rate was very low for the appearance of a crystalline phase from the glassy state by annealing. Even the degree of crystallinity was small, i.e. nearly 11%, the material became opaque as a result of the spherulitic superstructure. Saheb and co-workers [12] studied the crystallization and equilibrium melting behaviour of PBT/PETG blends. A single composition dependent glass transition temperature was observed. Papadopoulou and co-workers [13,14] studied the compatibility behaviour of PETG blended with PET or PBT over complete composition range. It was found that the PBT/PETG blends exhibited miscibility in the amorphous state as evidenced by the single composition dependent glass transition temperature and enhanced properties due to interaction between the two polymers and the PET/PETG blends were miscible when the PETG content is more than 50 vol%. Karger-Kocsis et al. [15] reported stress oscillation phenomenon in the necking phase of cold drawn amorphous copolyester. Karger-Kocsis and co-workers [16,17] investigated the fracture toughness of an amorphous copolyester by the essential work of fracture concept using tensile-loaded deeply double-edge notched specimens. It was established that both specific essential and non-essential work of fracture are composed of terms linking to yielding and necking, respectively. The essential work was likely to be independent of the thickness range when plane stress conditions prevail, and thus represented a material parameter. The essential work also did not change with increasing deformation rate. Ching and co-workers [18] studied the effects of gauge length and strain rate on fracture toughness of the PETG film using the essential work of fracture analysis. Hwang and co-workers [19] reinforced the PETG with a liquid crystal polymer (LCP) consisting of PET (40%) and polyhydroxy benzoic acid (60%). It was shown that the tensile strength and modulus of PETG were greatly improved with increasing LCP content, whereas, the elongation at break showed a reverse trend. The interfacial adhesion between the two components was poor. Handa et al. [20] reported the results on PETG foams by using CO_2 as blowing agent. PETG has a high affinity for CO_2, and was easily processed into foams of varying cell sizes.

Few literatures concerned toughening of the PETG plastic before. Actually, it is a pseudo-ductile polymer characterized by high crack initiation energy and low crack propagation energy, and consequently, by high un-notched and low notched impact strength. Its notched impact strength at ambient temperature and dry state is just 23.5 J/m [21]. In a previous work [21], the PETG was super-toughened by using the TPEg toughener. A sharp transition from brittle to ductile took place when the TPEg content was about 10 wt%. A similar transition was also observed for the PETG/POEg blends, but the POEg content for the transition was higher, i.e. 15 wt%. The TPEg showed a higher toughening efficiency than the POEg because of its better dispersion in the PETG matrix than that of the POEg.

The TPEg pellets are usually in yellow or bright-brown colour due to the maleic anhydride grafting via a reactive extrusion process. When it is used to fabricate a polymer material product by blending with other polymer component(s), it will inevitably colour the polymer material product. Therefore, the purpose of this study is to minimize the TPEg content in a super-toughened polymer material. This paper is concerned with toughening of the PETG plastic by blending with both the TPEg and its non-grafted version (TPE). The compatibilizing and toughening effects of the TPEg on the PETG/TPE blends are examined.

2. Experimental

2.1. Materials

The amorphous copolyester of ethylene glycol, 1,4-cyclohexanedimethanol and terephthalic acid with a molar ratio of approximately 1:2:3 [11], is a commercial product of Eastman Chemical Company (Rochester, NY) under the trade name of Eastar PETG 6763. Its intrinsic viscosity and glass transition temperature are 0.73 dl/g and 81 °C, respectively. The POE is a commercial product of Dupont Dow Elastomers (DE, USA) under the trade name of Engage 8445. Its octene content and melt flow index are 9.5 wt% and 3.5 g/10 min, respectively. The melting peak of the POE is very large, ranging from 25 to 80 °C, and its crystallinity is 12.6%. A maleated TPEg was prepared by maleic anhydride grafting of a mixture of POE elastomer/semi-crystalline polyolefin (60/40 by weight) in a twin-screw extruder (SHJ-30, China) with a 30 mm diameter and an *L*/*D* ratio of 23.2. The grafting ratio of maleic anhydride is about 1% by weight. The corresponding non-grafted mixture was also prepared and designated as TPE.

2.2. Blend preparation

The PETG was blended with a mixture of TPE and TPEg. Prior to blending, the PETG was dried at 70 °C under vacuum for 6 h. Blends were prepared in the extruder at 85 wt% of PETG plus 15 wt% of TPE/TPEg mixture ranging from 0 to 100 wt% of TPEg at five different

intervals. The amount of maleation in the dispersed phase was varied by dilution of TPEg with its non-grafted version TPE. The screw speed and the barrel temperatures of the extruder were 240 rpm and 225–245 °C, respectively. The extruded materials were dried and injection moulded into standard tensile, flexural, and Izod impact specimens in an injection-moulding machine (SZ-160/80 NB, China).

2.3. Mechanical testing

The tensile and flexural tests were carried out on an Universal Tensile tester (Instron 1122) according to the National Standard Test Methods of China, GB 1040-79 and GB 1042-79, respectively. They are very similar in sample dimensions and test conditions to ASTM D638 and ASTM D790, respectively. The notched Izod impact strength was measured at an ambient temperature using an impact tester (CSI-127C, USA) according to National Standard Test Method of China GB 1843-80, which is similar to ASTM D256. For all these tests, at least five specimens were used for each measurement.

2.4. Molau solution test

Molau solution test [22–24] was used to investigate the compatibility between PETG and TPEg. 0.3 g of the PETG/TPEg (90/10) blend was mixed with 10 ml of tetrachloroethane/phenol (1:1 by volume/weight) solution. This solution is a solvent for PETG and a non-solvent for TPE and TPEg. The mixture was first shaken thoroughly in a tube and then left alone at room temperature for a long period. If the compatibility between two components is poor, the non-soluble component will separate and float on the solution. Then, the solution test result is called negative. On the other hand, if the blend has good compatibility, a colloidal suspension will arise, which means that the solution test is positive. The same procedure was repeated with blend of PETG/TPE (90/10).

2.5. Morphology observation and image analysis

To estimate the particle size of the TPE/TPEg dispersed phase in the PETG matrix and the morphology of the blends, the surfaces of freeze fractured specimen in liquid nitrogen and those of impact fractured specimens at room temperature were observed after they were gold-sputtered with a scanning electron microscope (SEM) (Hitachi S-530, Japan). A semi-automatic image analyser was used to measure the apparent diameter (a_i) of the dispersed phase, which was then converted into true particle diameter (d_i) [1]. Typically over 200 particles from different photographs of a specimen surface were analysed to calculate the number average diameter d_n, and volume average diameter d_v from the following relationships [25,26]

$$\bar{d}_n = \sum n_i d_i / \sum n_i \quad (1)$$

$$\bar{d}_v = \sum n_i d_i^4 / \sum n_i d_i^3 \quad (2)$$

where n_i is the number of particles having the true particle diameter d_i.

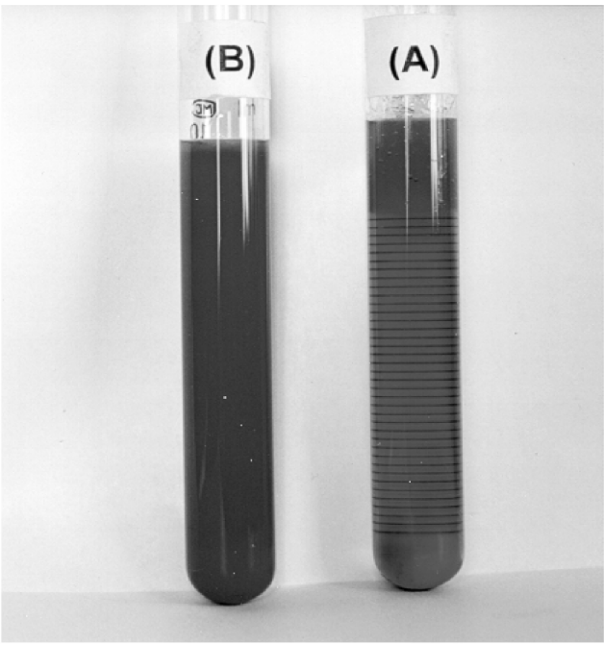

Fig. 1. Molau test solutions consisting of tetrachloroethane/phenol (1:1 by volume/weight) mixing solvents and each of the following blends: (A) PETG/TPE (90/10), (B) PETG/TPEg (90/10).

3. Results and discussion

3.1. Compatibilizing effect of the TPEg

Fig. 1 shows the results of Molau solution tests of PETG/TPE (90/10) blend and PETG/TPEg (90/10) blend in tetrachloroethane/phenol solvents. There was a phase separation in the solution containing the PETG/TPE (90/10) blend as shown in Fig. 1(A), the lower part of the tube (the clear area) being a clear solution consisting of PETG, and the upper part of the same tube (the vague area) being a suspension of TPE. It indicates that no chemical interaction took place between PETG and TPE during melt extrusion. Whereas Fig. 1(B) shows a colloidal suspension persisted in the solution containing the PETG/TPEg (90/10) blend, indicating the emulsification effect of the TPEg. It is believed that the maleic anhydride group of the TPEg reacts with the hydroxyl end group of the PETG to form a chemical linkage, forming an in situ generated PETG-*co*-TPEg copolymer during melt extrusion as shown below [27,28]:

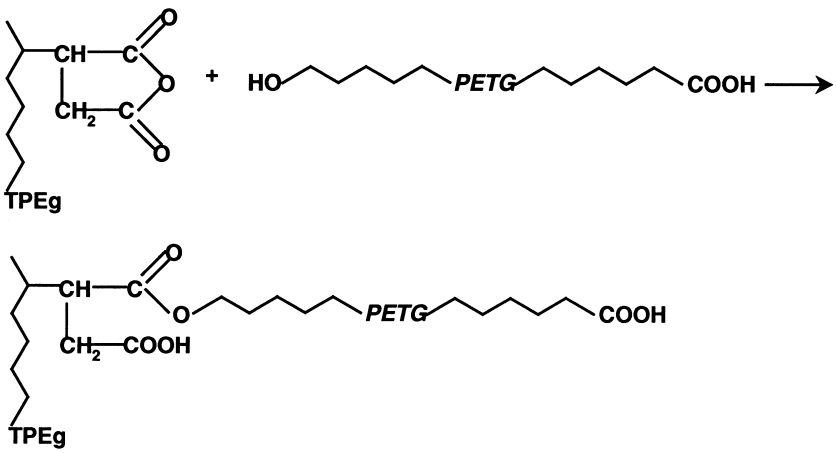

Tanrattanakul and co-workers [27] confirmed the chemical reaction between the PET and the maleic anhydride grafted styrene–ethylene/butylene–styrene tri-block copolymer (SEBS-*g*-MA) at high temperature. In their work, blends of PET with grafted SEBS-*g*-MA and non-grafted SEBS were extracted by tetrahydrofuran (THF) in an attempt to isolate an SEBS-*g*-MA component that had chemically reacted with PET. The THF is a good solvent for SEBS and SEBS-*g*-MA, but a non-solvent for PET. The THF-insoluble fraction were characterized by photo acoustic FTIR. They showed that The THF-insoluble fraction contained un-extracted SEBS-*g*-MA by strong absorbance of SEBS in the C–H stretching region. This un-extracted SEBS-*g*-MA had to be chemically linked to the PET in order not to be extracted by the THF solvent. The chemical reaction between maleic anhydride group and hydroxyl group was also demonstrated in PBT/ethylene–propylene rubber grafted maleic anhydride (EPR-*g*-MA) blend by Cecere and co-workers [28].

Fig. 2 shows the SEM photographs of freeze fractured surface of the PETG/TPEg/TPE blends with fixed dispersed phase content of 15 wt%. Fig. 3 gives the effects of TPEg content on number average and volume average diameters of the dispersed phase at the fixed content of the dispersed phase. Initially, the particle size rapidly decreases with increasing TPEg content. When the TPEg content in the dispersed phase is more than 50 wt%, the particle size seems to be unchangeable. An overall decrease of 3.2 times in the volume average diameter is shown. In addition, the particle size distribution, d_v/d_n, is reduced from 1.5 to 1.1, implying that the presence of the TPEg results in a more homogeneous dispersion of the TPE in the matrix. The fine dispersion of the dispersed phase upon incorporation of

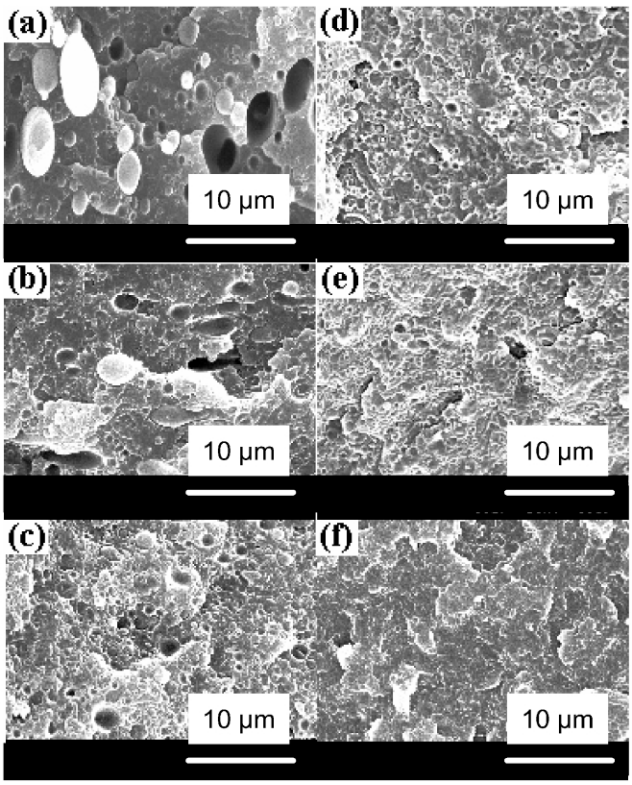

Fig. 2. SEM photographs of surfaces of freeze fractured PETG/TPEg/TPE blends with compositions of (a) 85/0/15, (b) 85/3/12, (c) 85/4.5/10.5, (d) 85/7.5/7.5, (e) 85/12/3, (f) 85/15/0, respectively.

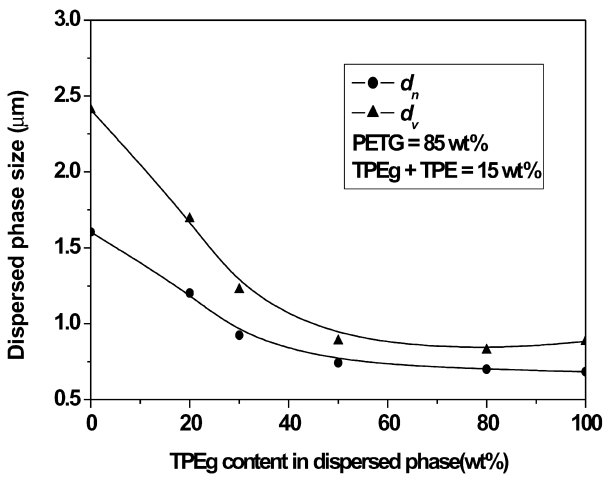

Fig. 3. Volume average diameter (d_v) and number average diameter (d_n) as a function of TPEg content in the dispersed phase for PETG/TPEg/TPE blends with a fixed dispersed phase content of 15 wt%.

an interfacial modifier is mainly caused by two different phenomena: a decrease in interfacial tension and a decrease in coalescence. Favis and co-workers [29,30] evaluated the relative roles of coalescence and interfacial tension in controlling dispersed phase size reduction during compatibilization based on both emulsification curves and interfacial tension measurements. They showed that in the case of the PET/PP (99/1) blend, upon addition of the SEBS-*g*-MA, the decrease of the dispersed phase size was caused only by a decrease in interfacial tension [30]. Whereas for PET/PP (90/10) blend, both lowering of interfacial tension and suppression of coalescence were equally important in determining the reduction of dispersed phase size during compatibilization [30]. It is believed that, in the present PETG/TPE blends, the TPEg acts as a compatibilizer to lower the interfacial tension between PETG and TPE and suppress the tendency of coalescence, and thus improves dispersion of the TPE particles. Simultaneously it also enhances interfacial adhesion between the components.

3.2. Toughening effect of the TPEg

Fig. 4 shows the effects of TPEg content in the dispersed phase on notched Izod impact strength and yield strength of PETG/TPEg/TPE blends with a fixed dispersed phase content of 15 wt%. When the TPEg content in the dispersed phase is 0 wt%, namely that the dispersed phase totally consists of the TPE, the impact strength is very low and the blend is brittle. This is due to poor compatibility between polar PETG and non-polar TPE. 20 wt% of TPEg in the dispersed phase results in slight increase in impact strength, the blend is still brittle. However, when the TPEg content in the dispersed phase is increased from 20 to 30 wt%, a sharp brittle–ductile transition occurs and the impact strength increases by more than twenty folds. After the transition, further increase in the amount of the TPEg does not result in a large change in impact strength. Since it is widely

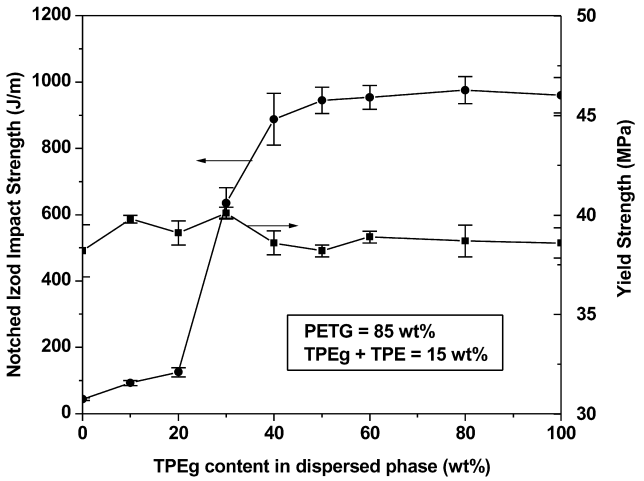

Fig. 4. Notched Izod impact strength and yield strength as a function of TPEg content in the dispersed phase for PETG/TPEg/TPE blends with a fixed dispersed phase content of 15 wt%.

accepted that notch Izod impact strength value greater than 530 J/m is regarded as super-tough [1], the PETG/TPE blends were super-toughened by addition of the TPEg. At 15 wt% of dispersed phase content, the minimum TPEg content (χ) for super-toughening PET/TPEg/TPE [85/χ/(15 − χ)] blends is $\chi = 4.5\%$. Whereas, in the binary PETG/TPEg blending system, the minimum TPEg content for making PETG super-tough is 10 wt% [21].

As demonstrated in many polymer/elastomer blending systems, the brittle–ductile transition is controlled by critical surface-to-surface interparticle distance (τ_c). The mechanism appears to involve the cavitation of elastomer particles, which relieves the hydrostatic stresses, and thus allows thin matrix ligaments ($\tau < \tau_c$) to yield locally [1]. When the thin matrix ligaments are interconnected to form a pervasive network, the yielding process can then propagate and pervade over the entire deformation zone. When this occurs, the blend will exhibit a ductile behaviour. Till now, the τ_c values shown in literatures are 0.3 μm for nylon 66/EPDM-*g*-MA blends [1,31], 0.15 μm for isotactic PP/EPDM blends [32], 0.33 μm for PBT/POE-*g*-MA blends [8], 0.6 μm for both HDPE/EPDM and HDPE/calcium carbonate blends [33,34], and 0.44 μm for PETG/rubber blends [35].

The τ_c for the onset of a brittle–ductile transition is directly related to both content and average diameter of the dispersed phase as shown below [1]

$$\tau_c = d_c\{[\pi/(6\phi_d)]^{1/3} - 1\} \quad (3)$$

where d_c is the critical dispersed particle diameter, ϕ_d is the volume fraction of the dispersed phase. ϕ_d is calculated by [1]

$$\phi_d = \rho_m\omega_d/\{(\rho_m - \rho_d)\omega_d + \rho_d\} \quad (4)$$

where ρ_m and ρ_d are the densities of matrix and dispersed phase, respectively. ω_d is the weight fraction of dispersed phase. The density of the PETG is 1.27 g/cm^3 and that of the TPE is 0.89 g/cm^3. Assuming the effect of the maleic anhydride, grafting on the density of the TPE is negligible because of the low grafting ratio. The density of the TPEg is believed to be the same as that of the TPE. $\omega_d = 0.15$ corresponds to $\phi_d = 0.202$. Hence, the critical dispersed particle size d_c for the onset of the brittle–ductile transition of the PETG/TPEg/TPE [85/χ/(15 − χ)] blends was calculated and it is approximately 1.18 μm. Fig. 5 shows the plot of impact strength from Fig. 4 versus the number average diameter from Fig. 3. It is seen that the impact strength has a sharp brittle–ductile transition when the diameter is reduced from 1.2 to 0.92 μm. The calculated value of $d_c = 1.18$ μm for the onset of the brittle–ductile transition of the PETG/TPEg/TPE blends seems to be reasonable. The brittle–ductile transition at a critical diameter d_c for a fixed dispersed phase was also found in nylon 6 and nylon 66 blends [1,4,36].

Although the values of notched impact strength show a sharp transition with varying levels of the TPE and the TPEg

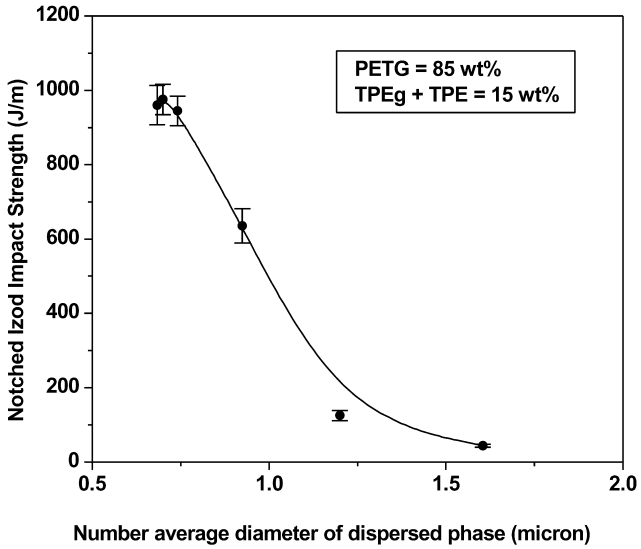

Fig. 5. Notched Izod impact strength as a function of number average diameter of the dispersed phase for PETG/TPEg/TPE blends with a fixed dispersed phase content of 15 wt%.

at a given dispersed phase content, other mechanical properties of the blends, such as yielding strength, flexural strength and modulus do not change much as shown in Figs. 4 and 6. It indicates that the tensile strength, flexural strength, and modulus are not sensitive to the changes of the particle size of dispersed phase and the compatibility in this blending system. The less dependence of improved compatibility on low strain tensile and flexural properties was shown in many literatures [7,8]. Whereas, in nylon 66/SEBS/SEBS-*g*-MA blends, the yielding strength and tensile modulus decrease continuously as the fraction of SEBS-*g*-MA increases for a fixed rubber content [4].

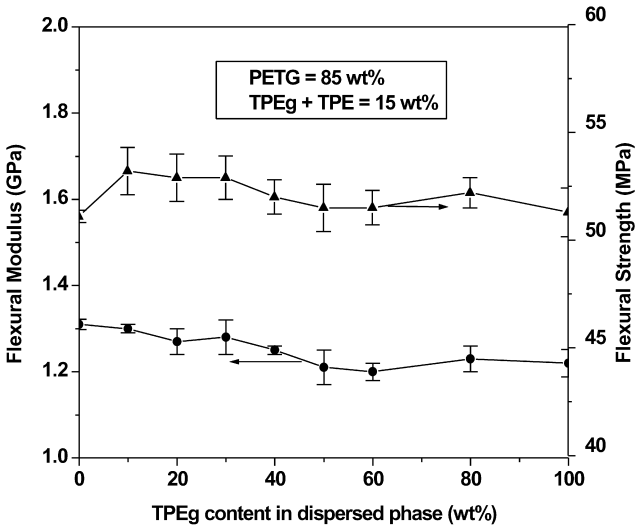

Fig. 6. Flexural modulus and flexural strength as a function of TPEg content in the dispersed phase for PETG/TPEg/TPE blends with a fixed dispersed phase content of 15 wt%.

3.3. Fractography

The impact fracture processes of a solid polymer material are well reflected in the appearance of the fracture surface [37–42]. Observation of the fracture surface helps us to understand the involved impact energy dissipation mechanisms upon impact testing. Fig. 7 shows the SEM fractographs of the impact fractured surfaces of the PETG/TPE (85/15) blend. The fracture surface exhibits a region of slow crack growth (denoted as *S*) at the notch root followed by a region of fast crack growth (denoted as *F*) as shown in the low magnification fractographs (Fig. 7(a) and (b)). The slow crack growth region is near the notch root. In this region, the crack propagation is believed to be slow because of the blunt notch produced before impact testing. At high magnification, the slow crack growth region, as shown in Fig. 7(c), is smooth. Due to the poor compatibility between PETG and TPE, the interfacial adhesion between them is poor. The cavitation around the rubber particles is very limited and the fracture surface shows a brittle failure. When the crack reaches a critical length for the applied stress, it becomes unstable and propagates very rapidly and the higher stress is sufficient to actuate flaws well in advance of the main crack front. In other words, these flaws are activated by the advanced stress wave and become sources of the secondary cracks. In the fast crack growth region, the secondary cracks propagate radially from the flaws. The intersection of the main crack front with the secondary cracks on different planes generates a number of feather-like or parabolic markings, which are indicative of the secondary cracks. The formation of these markings is determined by both the main crack front rate and secondary crack

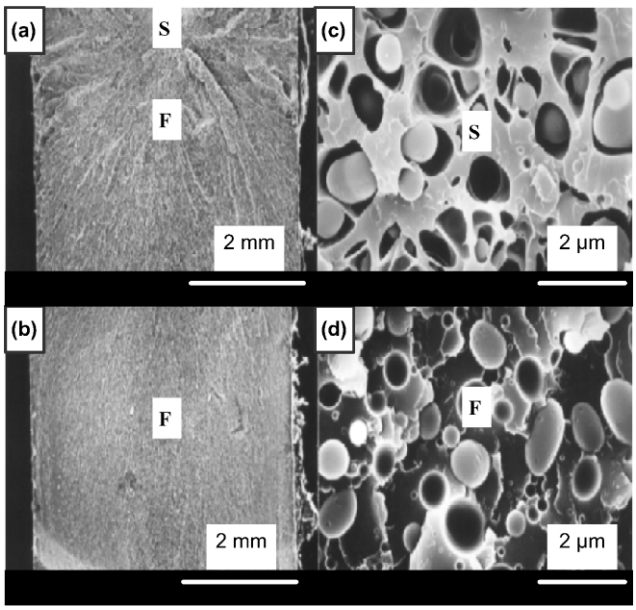

Fig. 7. SEM photographs of impact-fractured surface of PETG/TPE (85/15) blend under low (a,b) and high (c,d) magnifications. *S* and *F* denote the slow and fast crack growth regions, respectively.

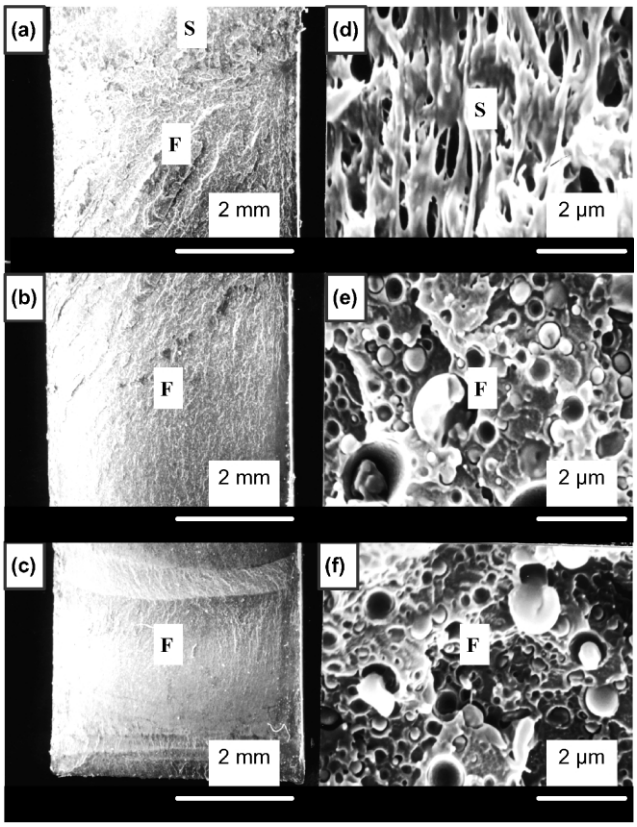

Fig. 8. SEM photographs of impact-fractured surface of PETG/TPEg/TPE (85/3/12) blend with a fixed dispersed phase content of 15 wt% under low (a–c) and high (d–f) magnifications. *S* and *F* denote the slow and fast crack growth regions, respectively.

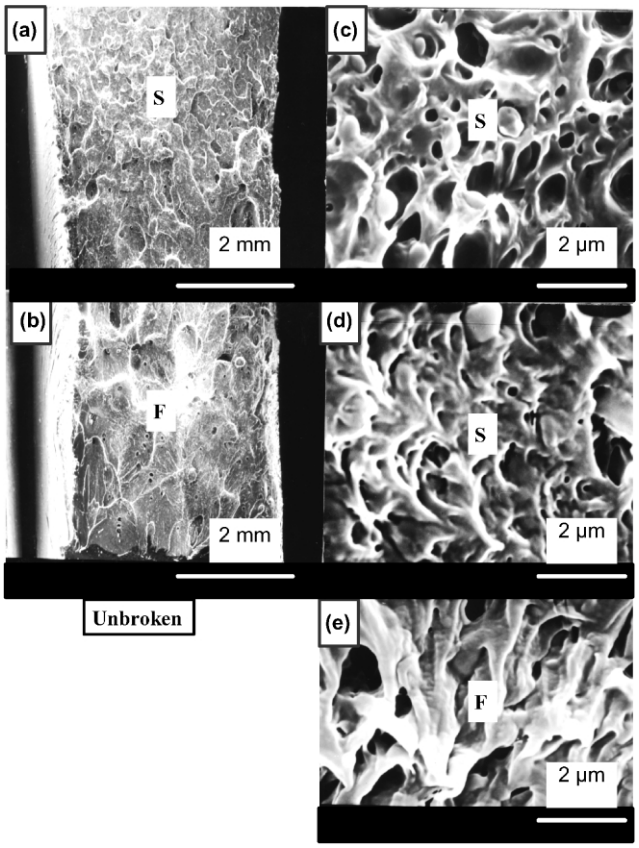

Fig. 9. SEM photographs of impact fractured surface of PETG/TPEg/TPE (85/4.5/10.5) blend with a fixed dispersed phase content of 15 wt% under low (a,b) and high (c–e) magnifications. *S* and *F* denote the slow and fast crack growth regions, respectively. The specimen did not break completely.

propagation rate [43,44]. The fast crack growth region of the PETG/TPE (85/15) blend exhibits a number of feather-like markings that are the classic fracture markings of brittle polymers as shown in Fig. 7(a) and (b). The high magnification graph of this region also shows smooth and brittle fracture feature.

Fig. 8 shows the SEM fractographs of the impact fracture surfaces of the PETG/TPEg/TPE (85/3/12) blend. As shown in the top of Fig. 8(a), the addition of 3 wt% of TPEg enlarges the area of the slow crack growth region. The large slow crack growth region corresponds to high impact strength. Under high magnification, cavitation and matrix shear yielding appear in this region as shown in Fig. 8(d), which would be the main contribution to the increased impact strength. However, its fast crack growth region still shows feather-like markings under low magnification (Fig. 8(a)–(c)). No matrix yielding appears in this region and the fracture surface looks smooth and shows brittle as shown in the high magnification graphs of Fig. 8(e) and (f). It should be noted that 3 wt% of the TPEg really decreases the particle size of the dispersed phase.

Continuously increasing the TPEg content to 4.5 wt% dramatically changes the fracture surface of the PETG blend. Fig. 9 shows the SEM fractographs of the impact fracture surfaces of the PETG/TPEg/TPE (85/4.5/10.5) blend. In low magnification photographs, the area of the slow crack region is greatly enlarged (Fig. 9(a)) and the fast crack growth region exhibits parabolic markings rather than feather-like ones. Each parabola contains a flaw at the focus, at which secondary fracture is initiated. At high magnification, both the slow and fast crack growth regions exhibit profuse cavitation and extensive matrix shear yielding. Now, it is generally believed that the shear yielding mechanism constitutes cavitation of the elastomer particles followed by shear yielding throughout the matrix [45–47]. The cavitation of the elastomer particles explains the observed stress whitening as light scattering occurs which is enhanced by the holes enlarging. Cavitation is followed by the onset of shear yielding, because on cavitation in the elastomer particles, the build up of hydrostatic tension is locally relieved and the yield stress is lowered. After cavitation, the constrained conditions, triaxial stresses, disappear and the matrix behaves as if it was under plane stress conditions. Shear yielding deformations occur more readily under a biaxial stress state rather than the craze-favouring triaxial state [45]. Although cavitation of the elastomer particles does involve energy absorption, the

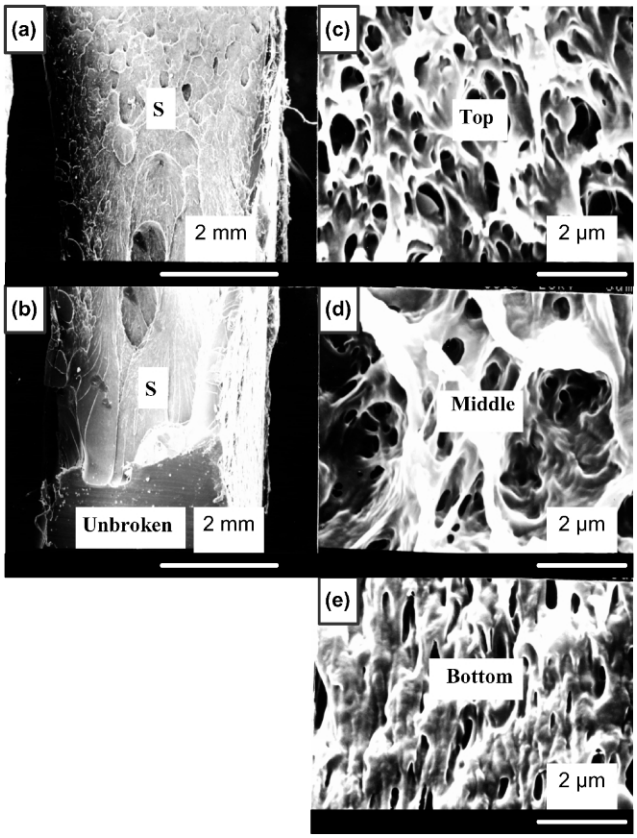

Fig. 10. SEM photographs of impact fractured surface of PETG/TPEg/TPE (85/7.5/7.5) blend with a fixed dispersed phase content of 15 wt% under low (a,b) and high (c–e) magnifications. The specimen did not break completely.

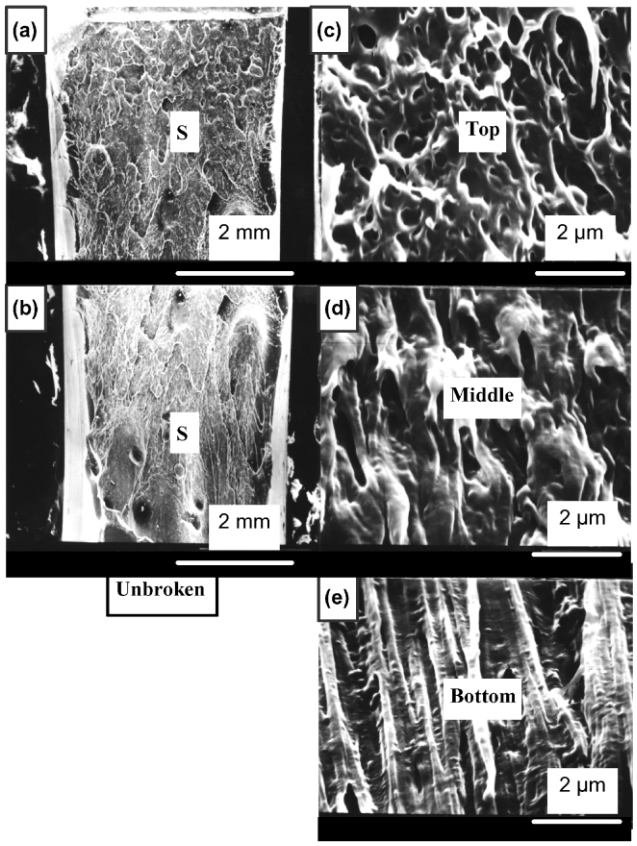

Fig. 11. SEM photographs of impact fractured surface of PETG/TPEg (85/15) blend under low (a,b) and high (c–e) magnifications. The specimen did not break completely.

enhanced shear yielding of the matrix is the major energy absorbing mechanism [45–47].

In addition, from the low magnification graphs of Fig. 9(a) and (b), lateral contraction of the sample sides and sub-surface whitening are visible, which are typical features of super-toughened polymer blends [48]. It is interesting to note that the presence of 4.5 wt% TPEg makes the PETG/TPE blend too tough to break completely under the severe notch impact testing. The drastic change of the fractography of the PETG/TPEg/TPE blend caused by increasing the TPEg content from 3 to 4.5 wt% is well in consistent with the brittle–ductile transition of the blend that occurred in the same TPEg content range.

On further increasing the TPEg content in the dispersed phase, the matrix shear yielding is more extensive. Fig. 10 shows the SEM fractographs of the impact fracture surfaces of the PETG/TPEg/TPE (85/7.5/7.5) blend. The fracture surface is mainly occupied by slow crack growth region with some parabolic markings caused by secondary cracks. The blends were not broken completely and showed obvious lateral contraction of the sample sides. The top part adjacent to the notch root exhibits uniform and profuse cavitation and highly drawn matrix ligaments. The middle part of the fracture surface shows massive cavitation and matrix shear yielding. The elongated cavitation and the extensive matrix plastic flow appear in the bottom part of the fracture surface. Fig. 11 shows the SEM fractographs of the impact fractured surfaces of the PETG/TPEg (85/15) blend. The fracture surface is similar to that of the PETG/TPEg/TPE (85/7.5/7.5) blend in Fig. 10. One small difference is that in Fig. 11, the matrix plastic flow was more intensive and the matrix was stretched to many parallel fibrils along the fracture direction as shown in Fig. 11(e).

4. Conclusions

The maleic anhydride grafting of TPE enhances the compatibility of the PETG/TPE blends and improves the dispersion of TPE in PETG matrix. At a fixed dispersed phase content of 15 wt%, a sharp brittle–ductile transition takes place when the TPEg content in the dispersed phase increases from 20 to 30 wt%. Further increasing the TPEg content does not clearly change the notched impact strength and the blends remain at a super-tough level. The minimum TPEg content (χ) for super-toughening PET/TPEg/TPE [85/χ/(15 − χ)] blends is $\chi = 4.5\%$. Whereas, in the binary

PETG/TPEg blending system, the minimum TPEg content for making the PETG super-tough is 10 wt%.

The fractography of the impact fracture surfaces of the PETG/TPEg/TPE blends shows a drastic change when the TPEg content in dispersed phase is in a range of 20–30 wt%. Before the brittle–ductile transition of the blends, the impact fracture surface exhibits a small area of slow crack growth region and numerous feather-like markings in fast crack growth region, indicating a brittle failure mode. After the brittle–ductile transition, the impact fracture surface exhibits greatly enlarged slow crack growth region and some parabolic markings in the fast crack growth region. Massive cavitation and extensive matrix shear yielding are two predominant mechanisms of the impact energy dissipation upon impact testing.

References

[1] Wu S. Polym Engng Sci 1990;30:753.
[2] Borggreve RJM, Gaymans RJ, Schuijer J, Housz JFI. Polymer 1987; 28:1489.
[3] Muratoglu OK, Argon AS, Cohen RE, Weinberg M. Polymer 1995; 36:921.
[4] Oshinski AJ, Keskkula H, Paul DR. Polymer 1992;33:284.
[5] Tomova D, Kressler J, Radusch HJ. Polymer 2000;41:7773.
[6] Papadopoulou CP, Kalfoglou NK. Polymer 2000;41:2543.
[7] Tanrattanakul V, Hilter A, Baer E, Perkins WG, Massey FL, Moet A. Polymer 1997;38:4117.
[8] Arostegui A, Gaztelumendi M, Nazabal J. Polymer 2001;42:9565.
[9] Yu ZZ, Ou YC, Qi ZN, Hu GH. J Polym Sci, Part B: Polym Phys 1998;36:1987.
[10] Yu ZZ, Lei M, Ou YC, Hu GH. J Polym Sci, Part B: Polym Phys 1999; 37:2664.
[11] Kattan M, Dargent E, Ledru J, Grenet J. J Appl Polym Sci 2001;81: 3405.
[12] Saheb DN, Jog JP. J Polym Sci, Part B: Polym Phys 1999;37:2439.
[13] Papadopoulou CP, Kalfoglou NK. Eur Polym J 1997;33:191.
[14] Papadopoulou CP, Kalfoglou NK. Polymer 1997;38:631.
[15] Karger-Kocsis J, Czigany T, Moskala EJ. Polym Engng Sci 1999;39: 1404.
[16] Karger-Kocsis J, Czigany T, Moskala EJ. Polymer 1998;39:3939.
[17] Karger-Kocsis J, Czigany T, Moskala EJ. Polymer 1998;39:4587.
[18] Ching ECY, Li RKY, Mai YW. Polym Engng Sci 2000;40:310.
[19] Hwang SH, Jeong KS, Jung JC. Eur Polym J 1999;35:1439.
[20] Handa P, Wong B, Zhang Z, Kumar V, Eddy S, Khemani K. Polym Engng Sci 1999;39:55.
[21] Yu ZZ, Lei M, Ou YC, Yang GS, Hu GH. J Polym Sci, Part B: Polym Phys 2000;38:2801.
[22] Molau GE. J Polym Sci, Part A 1965;3:4235.
[23] Illing GA. Makromol Chem 1981;95:83.
[24] Yu ZZ, Ou YC, Hu GH. J Appl Polym Sci 1998;69:1711.
[25] Oshinski AJ, Keskkula H, Paul DR. Polymer 1996;37:4891.
[26] Carte TL, Moet A. J Appl Polym Sci 1993;48:611.
[27] Tanrattanakul V, Hiltner A, Baer E, Perkins WG, Massey FL, Moet A. Polymer 1997;38:2191.
[28] Cecere A, Greco R, Ragosta G, Scarinzi G, Taglialatela A. Polymer 1990;31:1239.
[29] Cigana P, Favis BD, Jerome R. J Polym Sci, Part B: Polym Phys 1996; 34:1691.
[30] Lepers JC, Favis BD, Tabar RJ. J Polym Sci, Part B: Polym Phys 1997;35:2271.
[31] Muratoglu OK, Argon AS, Cohen RE. Polymer 1995;36:2143.
[32] Li Q, Zheng WG, Qi ZN, Zhu XG, Choy CL. Sci Chin (Ser B) 1993; 36:16.
[33] Bartczak Z, Argon AS, Cohen RE, Weinberg M. Polymer 1999;40: 2331.
[34] Bartczak Z, Argon AS, Cohen RE, Weinberg M. Polymer 1999;40: 2347.
[35] Wu S. J Appl Polym Sci 1988;35:549.
[36] Oshinski AJ, Keskkula H, Paul DR. Polymer 1996;37:4909.
[37] Tjong SC, Ke YC. Polym Engng Sci 1996;36:2626.
[38] Pearson RA, Yee AF. J Mater Sci 1991;26:3828.
[39] Yu ZZ, Ke YC, Ou YC, Hu GH. J Appl Polym Sci 2000;76:1285.
[40] Hale W, Keskkula H, Paul DR. Polymer 1999;40:3353.
[41] Pawlak A, Perkins WG, Massey FL, Hiltner A, Baer E. J Appl Polym Sci 1999;73:203.
[42] Wong SC, Mai YW. Polymer 1999;40:1553.
[43] Newman SB, Wolock I. J Appl Phys 1958;29:49.
[44] Wolock I, Kies JA, Newman SB. In: Averbach BL, Felbeck DK, Hahn GT, Thoms DA, editors. Fracture. New York: Wiley; 1959. p. 250–62.
[45] Yee AF, Pearson RA. J Mater Sci 1986;21:2462.
[46] Pearson RA, Yee AF. J Mater Sci 1986;21:2475.
[47] Borggreve RJM, Gaymans RJ, Eichenwald HM. Polymer 1989;30:79.
[48] Hobbs JJ, Bopp RC, Watkins VH. Polym Engng Sci 1983;23:380.